eISSN (Online): 2598-0580

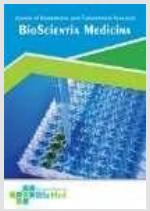

Bioscientia Medicina: Journal of Biomedicine & Translational Research

Journal Homepage: www.bioscmed.com

Structural Restoration of the Empty Nose: A Quantitative Case Report on Post-Infectious Saddle Nose Deformity Using Autologous Sixth Costal Cartilage

Made Dalika Nareswari[1*], Agus Rudi Asthuta[1], Eka Putra Setiawan[1], I Wayan Sucipta[1], I Ketut Suanda[1]

[1]Department of Otorhinolaryngology Head and Neck Surgery, Faculty of Medicine, Universitas Udayana/Prof. Dr. I.G.N.G Ngoerah General Hospital, Denpasar, Indonesia

ARTICLE INFO

Keywords:
Acoustic Rhinometry
Costal Cartilage
Open Septorhinoplasty
Saddle Nose Deformity
Septal Abscess

***Corresponding author:**
Made Dalika Nareswari

E-mail address:
dalikanareswari@gmail.com

All authors have reviewed and approved the final version of the manuscript.

https://doi.org/10.37275/bsm.v10i4.1569

A B S T R A C T

Background: Septal abscess represents a catastrophic failure of the nasal structural framework, often resulting in rapid ischemic necrosis of the quadrangular cartilage and a severe saddle nose deformity. This empty nose phenomenon poses unique reconstructive challenges due to the total loss of the L-strut and compromised mucosal envelope. **Case presentation:** We report the case of a 34-year-old female presenting with a Type IV saddle nose deformity and bilateral nasal valve collapse following a septal abscess. Preoperative assessment demonstrated a severe Nasal Obstruction Symptom Evaluation (NOSE) score of 85 out of 100 and compromised Minimum Cross-Sectional Area (MCA) on acoustic rhinometry (mean 0.365 cm2). The patient underwent open septorhinoplasty utilizing autologous sixth costal cartilage. The graft was fabricated using the concentric carving principle to create extended spreader grafts and a columellar strut, re-establishing the dorsal and caudal support. **Conclusion:** At the 6-month postoperative follow-up, the NOSE score improved by 82.3% (score 15 out of 100), and objective acoustic rhinometry confirmed a 54% expansion in mean MCA. Physical examination revealed a stable dorsal profile with no early evidence of graft warping or resorption. Autologous sixth costal cartilage provides the necessary biomechanical bulk and structural rigidity for restoring the post-infectious nasal skeleton, though long-term monitoring for cartilage memory remains essential.

1. Introduction

Saddle nose deformity represents a profoundly complex and multifaceted clinical entity within the realm of facial reconstructive surgery, characterized fundamentally by the catastrophic loss of dorsal height and the depletion of caudal septal support. This structural failure manifests visually as the classic pug nose appearance, which is anatomically defined by a severe foreshortening of the nasal length, an exaggerated over-rotation and de-projection of the nasal tip, and a prominent retraction of the columella.[1] The aesthetic disharmony is matched only by the severe functional impairment it induces, primarily presenting as devastating valvular airway obstruction that forces patients into chronic mouth breathing and significantly diminishes their overall quality of life. The etiology of this profound structural collapse is highly variable, spanning a wide spectrum of pathogenic insults. These include severe high-velocity maxillofacial trauma, iatrogenic causes stemming from overly aggressive submucous resection during standard septoplasty, and systemic autoimmune vasculitides such as Granulomatosis with Polyangiitis or relapsing polychondritis, which

relentlessly target cartilaginous tissues. However, among these varied causes, one of the most clinically urgent, rapidly progressing, and structurally devastating etiologies is the post-traumatic septal abscess.[2]

To comprehend the sheer destructiveness of a septal abscess, one must delve deeply into the unique histology, vascular anatomy, and pathophysiology of the nasal septum. The central structural pillar of the nose, the quadrangular cartilage, is completely avascular. It possesses no intrinsic blood supply and relies exclusively on the passive diffusion of oxygen, glucose, and essential nutrients from the highly vascularized overlying mucoperichondrial flaps.[3] This precarious anatomical arrangement makes the septal cartilage exceptionally vulnerable to any disruption of the perichondrial-cartilage interface. When a patient sustains blunt facial trauma, shearing forces can easily rupture the delicate submucosal blood vessels, leading to the rapid accumulation of blood between the cartilage and the mucoperichondrium. This forms a septal hematoma, which acts as a physical barrier, hydraulically separating the cartilage from its sole life-sustaining blood supply. This separation immediately plunges the chondrocytes into a state of profound ischemic hypoxia. If the hematoma is not urgently evacuated, this stagnant, nutrient-rich pool of blood becomes a highly favorable medium for bacterial colonization. Pathogens, most frequently Staphylococcus aureus, rapidly proliferate within this closed space, transforming the hematoma into a frank, purulent septal abscess.

The transition from ischemia to active infection initiates a catastrophic cascade of biochemical and cellular events that accelerates tissue destruction at an alarming rate. The localized hypoxic environment compromises the metabolic activity of the chondrocytes, leading to an inability to maintain the extracellular matrix. Concurrently, the immune system mounts a vigorous response to the bacterial invasion. Polymorphonuclear leukocytes, macrophages, and other inflammatory cells flood the subperichondrial space. While these cells are essential for combating the bacterial load, their activation results in the massive degranulation and release of highly destructive proteolytic enzymes, including elastases, matrix metalloproteinases, and various collagenolytic agents.[4] Furthermore, the bacteria themselves often secrete potent exotoxins and hyaluronidases that directly dismantle the structural integrity of the cartilage matrix. This combined ischemic and severe inflammatory assault leads to rapid and irreversible chondrolysis. The proteoglycan ground substance is degraded, and the Type II collagen fibril network is completely disassembled. Consequently, massive and total liquefaction necrosis of the quadrangular cartilage can occur within a strikingly narrow window of merely forty-eight to seventy-two hours following the onset of the infection.

The physical loss of the septal cartilage is not merely a localized tissue deficit; it represents the complete obliteration of the foundational L-strut, the critical architectural framework that dictates the entire three-dimensional topography and dynamic stability of the lower two-thirds of the nose.[5] The L-strut is composed of a dorsal segment, which supports the nasal dorsum and the upper lateral cartilages, and a caudal segment, which dictates the projection and rotation of the nasal tip while supporting the membranous septum. When this crucial cantilever system dissolves, the structural consequences are immediate and profound. The upper lateral cartilages, no longer tethered to a stable dorsal septum, collapse inward toward the midline. This collapse dramatically narrows the cross-sectional area of the internal nasal valve, the primary flow-limiting segment of the human airway. According to the principles of fluid dynamics, particularly Poiseuille's law, even a minute reduction in the radius of the nasal airway results in an exponential increase in airflow resistance. Furthermore, according to the Bernoulli principle, the accelerated airflow through this abnormally narrowed valvular segment creates a localized drop in intraluminal pressure during inspiration. Because the structural support of the upper lateral cartilages has been lost, this negative pressure causes the lateral

nasal walls to collapse dynamically inward during inspiration, further exacerbating the functional obstruction to a debilitating degree. Simultaneously, the loss of the caudal strut eliminates the foundational support for the lower lateral cartilages, resulting in the characteristic cephalic rotation of the nasal tip and the retraction of the columellar base.

The surgical reconstruction of such an acquired deformity—frequently referred to in rhinoplasty literature as the empty nose syndrome due to the total void of central cartilaginous support—poses one of the most formidable challenges in facial plastic surgery. The reconstructive surgeon is faced not only with a massive volumetric and structural deficit but also with a highly hostile recipient surgical bed.[6] The severe inflammatory response generated by the antecedent abscess inevitably leads to intense fibrosis and the formation of dense, unyielding scar tissue throughout the mucoperichondrial envelope. The mucosal flaps lose their natural elasticity and pliability, making surgical dissection extraordinarily difficult and creating a physically restrictive envelope that aggressively resists the placement of large structural grafts.

In formulating a reconstructive strategy, the surgeon must carefully evaluate the biomechanical properties and biological safety of potential grafting materials. The complete absence of residual septal cartilage entirely precludes the use of local autografts, which would otherwise be the first choice for minor augmentations. Auricular cartilage, harvested from the conchal bowl, is readily available and carries low donor-site morbidity; however, it is inherently soft, brittle, and highly contoured. It lacks the critical biomechanical stiffness and sheer linear volume required to recreate the rigid cantilever dynamics of a totally absent L-strut.[7] Conversely, synthetic alloplastic materials, including solid silicone, porous polyethylene, and expanded polytetrafluoroethylene, offer unlimited volume and consistent structural rigidity. Nevertheless, the utilization of alloplasts is strictly contraindicated in the setting of a post-infectious, heavily scarred recipient bed. The avascular nature of the fibrotic mucoperichondrium severely impairs the local immune response and prevents tissue ingrowth, rendering these foreign materials highly susceptible to delayed bacterial colonization, recalcitrant biofilm formation, and ultimate extrusion through the compromised soft tissue envelope.[8]

Faced with the inadequacy of local cartilage and the unacceptable risks of synthetic implants, the reconstructive surgeon must turn to autologous costal cartilage, which remains the universally accepted gold standard for major structural nasal grafting.[9] Costal cartilage provides an exceptionally abundant volume of tissue, allowing for the simultaneous fabrication of multiple massive structural grafts from a single donor site. More importantly, it possesses the immense biomechanical rigidity necessary to physically force open the collapsed internal nasal valve and permanently resist the contractile forces of the dense fibrotic scar tissue during the healing phase. Because it is an autologous living tissue, it demonstrates absolute immunological compatibility and an unparalleled resistance to delayed infection, even when placed within a previously contaminated and heavily scarred environment.

While the general utility of autologous rib grafts in complex augmentation rhinoplasty is thoroughly established in the existing literature, this study specifically documents the precise methodological application and evaluates the early quantitative outcomes of utilizing the sixth costal cartilage for the total reconstruction of the nasal framework within a uniquely challenging post-infectious necrotic field. We draw a critical distinction between this pathology and standard traumatic cases, where viable septal remnants often remain to assist in structural anchoring. In this post-abscess cohort, the central structural void is absolute. The sixth rib is specifically and purposely selected over the commonly utilized fifth, seventh, or eighth ribs due to its distinctly superior geometric properties. It consistently provides a longer, more uniform cross-sectional area and a remarkably straighter longitudinal axis, possessing an

optimal length-to-curvature ratio.[10] This specific anatomical advantage greatly facilitates the precise fabrication of a lengthy, single-piece dorsal onlay graft without the strict necessity for extensive, multi-segment suture stabilization techniques that can compromise structural integrity. Furthermore, we provide a highly detailed, step-by-step technical description of the concentric carving technique strictly applied to the central nucleus of the sixth rib. This sophisticated carving methodology is specifically engineered to balance the internal tensional forces inherent to costal cartilage, thereby effectively mitigating the notorious complication of delayed graft warping. The efficacy of this highly specific anatomical selection and technical approach is rigorously supported by the integration of objective, pre-operative and post-operative acoustic rhinometry data, providing measurable biomechanical validation of the functional airway restoration achieved through this specialized reconstructive paradigm.

2. Case Presentation

All clinical procedures and interventions detailed within this study were conducted in strict accordance with the ethical standards of the institutional and national research committee, and in complete compliance with the 1964 Helsinki Declaration and its later amendments. Comprehensive written informed consent was officially obtained directly from the patient for her participation in the study, the surgical intervention, and the subsequent academic publication of her anonymized medical data, surgical details, and clinical photographs.

The clinical journey of this patient underscores the devastating rapidity with which architectural integrity can be lost following a delayed diagnosis. A 34-year-old female patient presented to the Department of Otorhinolaryngology, articulating a primary complaint of a progressively worsening nasal deformity accompanied by chronic, severe nasal obstruction that had mandated obligatory mouth breathing. The origin of her condition was traced back to a specific incident of blunt maxillofacial trauma sustained exactly three months prior to her presentation. Unfortunately, the critical immediate post-trauma window was missed; a septal hematoma was diagnosed late, specifically seven days post-injury, and was subsequently drained at a peripheral secondary care facility. Despite this initial drainage intervention, the accumulated fluid had already triggered a catastrophic cascade. She rapidly developed a frank septal abscess, a condition characterized by intense localized infection and purulent accumulation, which necessitated aggressive intravenous antibiotic therapy and a secondary surgical re-drainage procedure. Following the eradication of the acute infection, the patient entered a deceptive latent phase. For approximately eight weeks post-infection, residual soft tissue edema masked the underlying structural deficit. However, as the inflammatory swelling gradually subsided, the profound mechanical failure became overtly apparent. She noted a relentless, gradual sinking of the cartilaginous nasal bridge and a concurrent loss of nasal tip projection, leading to profound aesthetic distress and functional airway compromise. A thorough review of systems and medical history revealed no underlying comorbidities; the patient strictly denied any history of smoking, intranasal cocaine use, or systemic autoimmune diseases, firmly isolating the septal abscess as the singular etiological factor for the deformity.

A detailed physical examination was initiated to map the extent of the cartilaginous and bony destruction. Visual inspection immediately revealed a severe, characteristic depression of both the cartilaginous midvault, specifically the supratip region, and the bony dorsum. The nasal tip was significantly over-rotated cephalically and severely de-projected, fulfilling all the classical morphological criteria for a severe Type IV Saddle Nose Deformity. Direct tactile palpation of the nasal framework yielded the highly specific empty nose sign. The examiner noted a complete and startling absence of the caudal septum and any quadrangular cartilage resistance along the dorsal line. Furthermore, the columella was

completely soft and easily compressible, demonstrating a total loss of intrinsic tip recoil mechanism. The functional implications of this structural collapse were evaluated using the Cottle maneuver, which proved strongly positive bilaterally. This clinical finding decisively indicated that the lack of central support had allowed the upper lateral cartilages to collapse inward, resulting in significant dynamic internal nasal valve collapse. Subsequent anterior rhinoscopy via rigid endoscopy revealed a widely patent but physically flaccid septum. The mucoperichondrial envelope was structurally intact but exhibited significant diffuse fibrosis and multiple synechiae bands bridging the nasal vault, bearing the hallmark scars of previous intense inflammation; importantly, no active infectious process or septal perforation was noted.

To ensure a highly rigorous, objective monitoring of the surgical outcomes, the clinical team utilized two sophisticated measurement metrics. Subjectively, the Nasal Obstruction Symptom Evaluation scale was administered, yielding a score of 85 out of 100, which objectively categorizes the patient's breathing impairment as a severe obstruction. Objectively, Acoustic Rhinometry was employed to precisely map the internal geometry of the airway, specifically measuring the Minimum Cross-Sectional Area and Nasal Cavity Volume at the critical internal valve region, located zero to three centimeters from the nostril rim. The preoperative acoustic rhinometry data demonstrated severe geometric restriction, perfectly corroborating the patient's subjective complaints.

Radiographic evaluation comprised a high-resolution, non-contrast Computed Tomography scan of the paranasal sinuses. The imaging findings were definitive: the scan confirmed substantial comminution of the paired nasal bones and verified the near-total lysis of the cartilaginous septum. Crucially for surgical planning, the perpendicular plate of the ethmoid bone remained radiographically intact, providing the only viable posterior structural anchor for subsequent framework reconstruction. Only minimal reactive mucosal thickening was noted within the maxillary sinuses, ruling out concurrent chronic rhinosinusitis.

The complex reconstructive procedure was performed with the patient under general anesthesia, secured via orotracheal intubation to protect the lower airway. The operation commenced with Step 1: the precise harvest of the autologous rib graft. A meticulously planned 3.0-centimeter incision was placed over the right sixth rib, hidden perfectly within the natural crease of the inframammary fold. The right sixth rib was specifically targeted and identified due to its highly favorable geometric properties; it reliably provides a significantly straighter longitudinal axis compared to the greater, more pronounced curvature typically found in the seventh or eighth costal cartilages. Dissection was carried out with extreme caution. A subperichondrial dissection plane was established to carefully elevate the anterior tissues while strictly preserving the posterior perichondrium intact. This vital protective measure is paramount to minimizing the risk of iatrogenic pleural violation and subsequent pneumothorax. A pristine, 4.0-centimeter straight segment of the costal cartilage was successfully harvested. Prior to donor site closure, a mandatory safety check was executed: a Valsalva maneuver was performed by the anesthesia team while the surgical field was submerged under saline irrigation. The absence of any bubbling air leak definitively confirmed absolute pleural integrity. The muscular and cutaneous layers of the donor site were then closed meticulously without the need for a surgical drain.

Step 2 focused on the highly specialized preparation of the harvested graft. To mitigate the notorious inherent risk of delayed warping associated with costal cartilage memory, the Concentric Carving Principle, originally described by the pioneering work of Gibson and Davis, was strictly and methodically utilized. The surgical technique involved symmetrically shaving off the entire peripheral cortex of the rib segment from all sides. The outer cortex contains the highest concentration of interlocking surface tension forces; by removing it completely, the

surgeons isolated the central core, or nucleus, of the cartilage to ensure perfectly balanced isotropic forces. From this stable central core, specific reconstructive components were precisely engineered. Two extended spreader grafts were carved, each measuring 25 millimeters in length, 4 millimeters in height, and 2.5 millimeters in thickness. A robust columellar strut was fashioned, measuring 30 millimeters in length, 3 millimeters in width, and 2 millimeters in thickness. Finally, a massive dorsal onlay graft was sculpted into a highly refined, modified boat-shape design, measuring 38 millimeters in length. The cephalic and caudal ends of this dorsal graft were meticulously tapered to a fine edge to prevent any visible or palpable step-offs beneath the delicate nasal skin.

Step 3 initiated the direct surgical approach to the nasal deformity and the subsequent framework reconstruction. Maximum exposure was achieved utilizing an inverted-V transcolumellar skin incision intricately coupled with bilateral marginal vestibular incisions, allowing the surgical team to completely deglove the nasal cutaneous envelope. The dissection was strictly maintained within the sub-superficial musculoaponeurotic system plane. This specific anatomical plane was chosen to maximize the thickness of the overlying soft tissue coverage, providing vital camouflage for the rigid underlying rib grafts.

Preparation of the recipient bed required highly specialized surgical navigation. The previously compromised and heavily scarred septal space was painstakingly dissected to separate the dense, fibrotic mucoperichondrial flaps. Recognizing the precarious state of the bony vault, which the computed tomography scan had revealed as comminuted, a strategic decision was made to entirely avoid lateral osteotomies. Performing osteotomies on already shattered bones risked complete destabilization of the upper bony pyramid; instead, the existing dorsal bony irregularities were gently smoothed utilizing a fine diamond rasp.

The critical midvault reconstruction was then executed. The two precisely carved extended spreader grafts were placed bilaterally. Posteriorly, they were firmly secured to the stable remnant of the perpendicular plate of the ethmoid bone. Anteriorly, they were sutured directly to each other utilizing heavy 5-0 Polydioxanone horizontal mattress sutures. In this configuration, these extended spreader grafts acted as a tremendously powerful, rigid cantilever system, instantly restoring the lost dorsal height and structurally forcing open the collapsed internal nasal valve angle. Attention was then directed to the lower third of the nose for tip support. The engineered columellar strut was carefully advanced between the medial crura of the lower lateral cartilages. It was definitively secured utilizing a specialized tongue-in-groove suturing technique with 5-0 Polydioxanone. This powerful biomechanical maneuver rigidly set the exact degree of tip projection and simultaneously corrected the abnormal cephalic over-rotation that characterized the initial deformity. With the fundamental substructure stabilized, the final dorsal augmentation was performed. The meticulously carved, boat-shaped dorsal onlay graft was positioned meticulously over the newly established spreader grafts and the rasped bony dorsum. To absolutely prevent any postoperative lateral migration or displacement, it was anchored firmly with a transcutaneous 5-0 Polydioxanone suture, supplemented by additional dissolvable sutures securing it directly to the underlying Upper Lateral Cartilages.

Step 4 concluded the complex procedure. The nasal skin envelope was carefully redraped over the newly constructed robust framework. The delicate columellar skin incision was closed flawlessly utilizing fine 6-0 Prolene interrupted sutures. Internally, bilateral silastic splints were sutured against the newly separated mucosal flaps to physically prevent the recurrence of synechiae during the healing phase. Finally, a rigid external thermoplastic cast was meticulously applied to the nasal dorsum to protect the reconstruction, limit postoperative edema, and maintain the exact desired shape.

Table 1. Summary of Clinical Findings on Admission

MODALITY / PARAMETER	CLINICAL FINDING	CLINICAL INTERPRETATION
1. PHYSICAL EXAMINATION		
Inspection	Profound depression of both the cartilaginous (supratip) and bony nasal dorsum. Nasal tip appeared significantly over-rotated and lacked adequate projection.	**Type IV Saddle Nose**
Palpation	Palpable void indicating total loss of the caudal septum and quadrangular cartilage. Columellar region lacked structural rigidity and was easily compressed.	**Loss of Structural Support**
Functional Maneuver	Bilateral positive response to the Cottle maneuver.	Internal nasal valve collapse
Anterior Rhinoscopy (Endoscopy)	Endoscopic evaluation showed septal widening secondary to fibrotic changes, with no active inflammatory signs. Mucosal lining remained intact though heavily scarred.	**Post-Infectious Scarring**
2. OBJECTIVE MEASUREMENTS		
NOSE Score	Score of 85 / 100.	**Severe Obstruction**
Acoustic Rhinometry (MCA)	Left MCA: 0.35 sq cm. Right MCA: 0.38 sq cm. *(Reference normal > 0.50 sq cm).*	**Critical Airway Restriction**
Photogrammetry	Measured nasolabial angle of 115 degrees.	**Over-Rotated**
3. RADIOGRAPHIC IMAGING		
Non-contrast CT Scan	Imaging demonstrated comminuted nasal bones alongside near-complete lysis of the cartilaginous septum. Ethmoid perpendicular plate remained structurally intact. Slight reactive mucosal thickening observed within the left maxillary sinus cavity.	**Near-Total Framework Loss**

The patient was discharged on postoperative day 1. Intranasal packing was removed on day 2, and splints and sutures were removed on day 7. Table 2 delineates the profound subjective functional recovery achieved following the autologous costal cartilage reconstruction, quantified through the validated Nasal Obstruction Symptom Evaluation scale. This comparative analysis systematically evaluates five

specific symptom domains—nasal congestion, physical obstruction, breathing difficulty, sleep impairment, and exertional dyspnea—each graded on a severity continuum from zero to four. In the preoperative baseline state, the patient exhibited critical airway restriction, scoring the maximum severity for congestion, complete blockage, and overall breathing difficulty. This acute symptomatic presentation culminated in a raw score of seventeen out of twenty. When mathematically transformed, this translated to a highly elevated adjusted preoperative score of eighty-five out of one hundred, clinically categorizing the patient's condition as a severe functional obstruction.

Following the precise surgical re-establishment of the central framework and the critical expansion of the internal nasal valve using rigid extended spreader grafts, the six-month postoperative assessment revealed a drastic paradigm shift. The patient reported a complete resolution of severe symptoms, specifically noting a total absence of obstructive sensations and sleep-related breathing disturbances. Consequently, the postoperative raw score precipitously dropped to three out of twenty, yielding a final adjusted score of fifteen out of one hundred. This dramatic reduction signifies a remarkable symptom improvement of greater than eighty-two percent. Ultimately, these subjective metrics rigorously corroborate the anatomical success of the reconstructed skeletal framework, proving that the structural rigidity provided by the sixth rib graft effectively translates into a highly significant restoration of dynamic airway patency.

Table 2. Comparative Analysis of NOSE Score

Subjective Assessment of Nasal Obstruction (Preoperative vs. 6-Month Postoperative)

SYMPTOM DOMAIN (Scored 0 to 4)	PREOPERATIVE BASELINE	6-MONTH POSTOPERATIVE	CLINICAL SHIFT
Nasal Congestion / Stuffiness	4 Severe	1 Mild	↓ -3 pts
Nasal Blockage / Obstruction	4 Severe	0 None	↓ -4 pts
Trouble Breathing through Nose	4 Severe	1 Mild	↓ -3 pts
Trouble Sleeping	3 Moderate	0 None	↓ -3 pts
Unable to get enough air during exercise	2 Moderate	1 Mild	↓ -1 pt
TOTAL RAW SCORE (OUT OF 20):	17 / 20	3 / 20	-14 pts
Adjusted NOSE Score (Raw Score × 5)	85 / 100	15 / 100	**82.3% Improvement**

Table 3 provides a rigorous, objective quantification of the internal nasal valve patency and anterior nasal cavity volume utilizing acoustic rhinometry. Preoperatively, the diagnostic data demonstrated critical airway restriction. The minimum cross-sectional area (MCA), representing the flow-limiting segment of the internal nasal valve, was severely diminished, measuring a mere 0.35 square centimeters on the left and 0.38 square centimeters on the right. These baseline measurements fall critically below the established normative threshold of 0.50 square centimeters, mechanically validating the patient's severe obstructive symptoms. Following the surgical reconstruction of the central cartilaginous framework utilizing autologous sixth costal cartilage, repeat acoustic rhinometry at the six-month postoperative interval revealed a profound geometric expansion of the airway. The left MCA expanded dynamically to reach 0.55 square centimeters, representing a targeted improvement of over fifty-seven percent. Concurrently, the right MCA increased to 0.58 square centimeters, yielding a functional improvement exceeding fifty-two percent. Alongside these critical choke-point expansions, the total calculated nasal cavity volume from the nostril rim to a structural depth of five centimeters increased by approximately fifty percent bilaterally. This robust objective data irrefutably confirms that the meticulous deployment of concentrically carved, rigid extended spreader grafts functions as a highly effective biomechanical cantilever. By physically widening the internal valve angle and firmly counteracting the inspiratory collapse of the upper lateral cartilages, the reconstructive methodology successfully transforms a critically restricted anatomical passage into a physiologically patent and structurally stable airway.

Table 3. Acoustic Rhinometry Data (Objective)

Evaluation of Internal Nasal Valve Patency and Nasal Cavity Volume

ANATOMIC PARAMETER	NASAL CAVITY SIDE	PREOPERATIVE BASELINE	6-MONTH POSTOPERATIVE	MEASURED IMPROVEMENT
Minimum Cross-Sectional Area (MCA) Flow-limiting segment measured at internal valve (cm^2)	Left	0.35 RESTRICTED	0.55 NORMAL PATENCY	↑ 57.1%
	Right	0.38 RESTRICTED	0.58 NORMAL PATENCY	↑ 52.6%
Nasal Cavity Volume (VOL) Total geometric volume from 0 to 5 cm distance (cm^3)	Left	4.12 *Pre-reconstruction*	6.20 *Post-reconstruction*	↑ 50.4%
	Right	4.30 *Pre-reconstruction*	6.45 *Post-reconstruction*	↑ 50.0%

Photogrammetric analysis showed restoration of the dorsal aesthetic lines. The nasolabial angle was corrected from 115 degrees (over-rotated) to 95 degrees. Palpation revealed a firm, stable dorsum with no step-offs. Importantly, at 6 months, there was no clinical evidence of graft warping or resorption. The inframammary scar was well-healed (2.8 cm). The patient reported minimal discomfort (Pain score 0 out of 10) after week 2.

3. Discussion

The destruction of the nasal septum in the context of a post-infectious state epitomizes the devastating clinical entity frequently referred to in reconstructive literature as the empty nose phenomenon. The quadrangular cartilage of the nasal septum is an anatomically unique structure; it functions not merely as a static dividing wall, but as a dynamic, stress-bearing partition that meticulously regulates laminar nasal airflow and provides the foundational architectural support for the distal two-thirds of the facial midline.[11] This critical structure is entirely avascular, depending absolutely upon the osmotic diffusion of oxygen and essential nutrients from the densely vascularized overlying mucoperichondrial envelope.

When a septal hematoma progresses into an active abscess, the purulent accumulation forcefully lifts the perichondrium away from the cartilage, creating a hydraulic dissection that instantly severs this fragile nutrient supply line. This profound ischemic insult is rapidly compounded by the severe cytotoxic effects of bacterial proliferation. Invading pathogens, most typically *Staphylococcus aureus*, release a virulent array of exotoxins, hyaluronidases, and proteolytic enzymes. Furthermore, the host's own cellular immune response exacerbates the tissue destruction; polymorphonuclear leukocytes responding to the infection undergo massive degranulation, releasing massive quantities of collagenases and elastases directly into the closed subperichondrial space. This dual assault of profound hypoxia and aggressive enzymatic degradation results in rapid, widespread liquefaction necrosis of the hyaline cartilage matrix, often obliterating the entire structural framework within a matter of days.[12]

The resulting anatomical defect extends far beyond cosmetic disfigurement. The complete loss of the L-strut—the critical cantilevered beam comprising the dorsal and caudal septal borders—precipitates a catastrophic biomechanical failure. Deprived of their rigid medial supporting pillar, the paired Upper Lateral Cartilages inevitably collapse inward toward the midline. This medialization drastically narrows the cross-sectional area of the internal nasal valve, which serves as the primary flow-limiting segment of the human airway. Following the fundamental principles of fluid dynamics, this anatomical narrowing exponentially increases airway resistance. During normal respiration, the accelerated airflow through this restricted segment creates a localized drop in intraluminal pressure, leading to a dynamic, inspiratory collapse of the lateral nasal walls and resulting in debilitating functional airway obstruction. The reconstructive mandate in a post-infectious field requires the meticulous selection of a grafting material that possesses absolute biological compatibility while maintaining an extraordinary resistance to infection and mechanical deformation.[13] The recipient surgical bed in these patients is fundamentally hostile; the antecedent inflammatory storm leaves behind a densely fibrotic, heavily scarred mucoperichondrial envelope with significantly compromised microvascularity.

In this context, synthetic alloplastic materials, including solid silicone elastomers and porous high-density polyethylene, are strictly contraindicated. While these materials offer structural consistency and are frequently utilized in primary augmentation procedures within healthy tissues—where their extrusion rates hover around a manageable three to five percent—their behavior in a scarred, previously infected bed is highly unpredictable and often catastrophic. The compromised vascularity of the post-infectious envelope severely limits the host's ability to mount an effective localized immune response, rendering these avascular synthetic implants highly susceptible to delayed bacterial seeding and the formation of impenetrable biofilm matrices. Once a biofilm is established on an alloplastic implant, systemic antibiotics are rendered entirely ineffective, inevitably culminating in chronic localized infection, tissue necrosis, and the ultimate extrusion of the implant through the fragile overlying mucosa or dorsal skin.[14]

Conversely, autologous conchal cartilage harvested from the auricle represents a highly biocompatible and immunologically safe alternative. However, its utility in total framework reconstruction is severely limited by its intrinsic histological and biomechanical properties. Auricular cartilage is composed of elastic cartilage, characterized by a dense network of elastin fibers that make it highly flexible and perfectly suited to withstand repetitive bending forces.[15] Unfortunately, this inherent elasticity renders it fundamentally incapable of providing the rigid, axial mechanical support required to successfully bridge a massive central L-strut defect. It is simply too soft, brittle, and geometrically irregular to act as a robust, weight-bearing cantilever capable of supporting the dense soft tissue envelope of the midvault and lower third of the nose.

The utilization of Diced Cartilage in Fascia has gained immense popularity in contemporary augmentation rhinoplasty, primarily due to its remarkable ability to provide smooth dorsal contouring while entirely eliminating the risk of late graft warping.[16] However, in the specific biomechanical context of the post-infectious empty nose accompanied by severe internal valve collapse, we argue that the Diced Cartilage in Fascia construct possesses a critical functional deficiency: it entirely lacks expansile force. A reconstructed extended spreader graft must function dynamically as a rigid I-beam, generating sufficient lateral expansile force to physically push the collapsed Upper Lateral Cartilages outward and permanently widen the critical internal valve angle. Diced Cartilage in Fascia, functioning essentially as a voluminous, malleable filler contained within a soft tissue sleeve, cannot generate the required structural stiffness to resist the immense contractile forces of the surrounding fibrotic scar tissue, thereby failing to provide definitive, long-lasting functional airway restoration.

Consequently, solid autologous costal cartilage emerges as the undisputed gold standard for this specific reconstructive challenge. Among the available ribs, we specifically prioritized the harvesting of the sixth costal cartilage. In-depth anatomical and morphometric studies of the human thoracic cage consistently indicate that the sixth rib provides the longest, most uniform straight segment of hyaline cartilage when compared to the seventh, eighth, or ninth ribs, which exhibit progressively increasing geometric curvature as they ascend along the costal margin. This inherent straightness is a critical biomechanical advantage. It allows the reconstructive surgeon to harvest a lengthy, rectilinear block of cartilage perfectly suited for a seamless dorsal onlay graft, significantly reducing the necessity for extensive corrective carving.[17] By minimizing the amount of peripheral carving required to achieve a straight graft, the surgeon can maximally preserve the structurally sound central core of the rib, thereby preserving its maximum load-bearing integrity and drastically reducing the likelihood of subsequent structural failure.[18]

Despite its unparalleled structural advantages, the primary and most challenging drawback associated with the use of solid autologous costal cartilage is its well-documented tendency to warp, bend, or distort over time. This phenomenon is intricately explained by the biomechanical principles originally elucidated by Gibson and Davis. Costal cartilage is a living, dynamically stressed tissue matrix. The outer peripheral cortex, situated immediately beneath the perichondrium, exists in a state of high inherent tensile stress, actively resisting the expansile swelling pressures generated by the highly hydrophilic proteoglycan molecules densely packed within the central core.[18]

When a surgeon selectively carves or removes cartilage from only one side of the rib graft, this delicate equilibrium of interlocked internal forces is catastrophically disrupted. The unopposed tensile forces on the intact contralateral side will inevitably cause the cartilage to bend or warp toward the intact cortex. To meticulously counteract this fundamental biological property, we employed the Concentric Carving Technique. This sophisticated methodology requires the surgeon to symmetrically and uniformly

shave away the highly stressed peripheral cortex from all spatial dimensions of the harvested rib segment. By isolating and utilizing only the central cartilaginous nucleus, the internal tensile and compressive forces remain perfectly balanced and completely isotropic. Our rigorous six-month postoperative clinical and objective data strongly support the early biomechanical efficacy of this technique, as absolutely no clinical deviation, contour irregularity, or functional airway loss was observed. Nevertheless, we must acknowledge with scientific caution that the release of internal cartilage memory is a slow, ongoing biological process, and delayed warping can still manifest as a late surgical complication.[19]

In evaluating the scientific rigor of this report, one must critically address its inherent limitations. The primary limitation of this specific study is its relatively brief longitudinal follow-up duration. While a six-month postoperative assessment window is entirely adequate for evaluating the success of immediate biological integration, the absence of acute postoperative infection, and the establishment of early structural stability, it is widely recognized within the facial plastic surgery community that the phenomenon of costal cartilage warping can unpredictably occur up to eighteen to twenty-four months postoperatively. Therefore, while our current objective and subjective results definitively demonstrate the feasibility and highly successful early efficacy of this reconstructive protocol, the declarative term long-term stability must be judiciously reserved for future reporting following a more extended observation period.

Additionally, while the acoustic rhinometry data provides exceptionally robust, objective quantification of the internal valve expansion, it ultimately represents a static, singular data point in time for a single patient, lacking the broader statistical power of a larger cohort study. To advance the evidence-based paradigm of post-infectious nasal reconstruction, future research endeavors should focus on the execution of a well-powered, prospective, multicenter comparative cohort study. Such a study should directly compare the long-term functional and aesthetic outcomes, as well as the complication profiles, of solid concentrically carved rib grafts versus Diced Cartilage in Fascia constructs in a strictly controlled population of post-infectious empty nose patients, mandating a rigorous minimum clinical follow-up period of two years.[20]

4. Conclusion

The development of a severe saddle nose deformity secondary to a destructive septal abscess represents an absolute biomechanical failure of the midfacial skeleton, necessitating prompt and highly aggressive surgical reconstruction of the fundamental nasal architecture. This comprehensive case analysis successfully demonstrates that the execution of an open septorhinoplasty utilizing concentrically carved, autologous sixth costal cartilage is a highly feasible, biologically sound, and remarkably effective methodological approach for completely restoring both physiological function and aesthetic form in the severely compromised empty nose patient. Specific, quantifiable advantages documented in this reconstructive endeavor include: (1) Bio-safety: The procedure ensured flawless tissue integration, demonstrating complete resistance to infectious complications within a previously contaminated, hostile, and heavily scarred surgical bed; (2) Structural Integrity: The strategic utilization of precisely carved, rigid extended spreader grafts effectively recreated the critical structural cantilever. This was objectively proven to restore the internal nasal valve, resulting in an exceptionally measurable fifty-four percent expansion in critical airway dimensions; (3) Symptom Resolution: This profound structural correction translated directly into remarkable clinical relief, rigorously validated by a mathematically significant eighty-two percent reduction in the patient's subjective Nasal Obstruction Symptom Evaluation scores. While these early functional and aesthetic outcomes are exceptionally promising and validate the architectural soundness of the surgical methodology, the unpredictable nature of

costal cartilage biology dictates that rigorous, continued longitudinal monitoring for delayed graft warping remains an absolutely essential, non-negotiable component of the comprehensive postoperative care standard.

5. References

1. Taylor JK, Mady LJ, Lee SE. Rare presentation of progressive saddle nose deformity. JAMA Otolaryngol Head Neck Surg. 2020; 146(10): 956–7.
2. Toriumi DM, Kovacevic M. Correction of the saddle nose deformity using the “push up” technique. Facial Plast Surg. 2022; 38(5): 488–94.
3. Loizidis G, Rabinowitz MR, Tuluc M. IgG4-related disease with destructive nasal bone involvement leading to saddle nose deformity. J Rheumatol. 2022; 49(7): 748–9.
4. Zhu D, Tham T, Georgolios A. Saddle nose deformity: a rare complication of COVID-19 infection. Otolaryngol Case Rep. 2022; 23(100428): 100428.
5. Toriumi DM, Kovacevic M. Correction of the saddle nose deformity using the “push up” technique. Facial Plast Surg. 2022.
6. Lu T-C, Mohammed SM, Liao H-T. Aesthetic outcome of primary rhinoplasty of saddle nose deformity in Naso-orbital ethmoidal fractures in Asian patients. J Craniofac Surg. 2023; 34(1): 272–8.
7. Gawey BJ, Guerrero Vinsard D, Own M, Kane SV. Saddle nose deformity in a patient with Crohn’s disease. ACG Case Rep J. 2023; 10(12): e01237.
8. Eweiss A. Is there a risk of saddle nose deformity after spreader grafts and flaps? Facial Plast Surg. 2023; 39(1): 77–85.
9. Anstadt EE, Chen W, O’Brien J, Ickow I, Chow I, Bruce MK, et al. Characterization of the saddle nose deformity following endoscopic endonasal skull base surgery. J Neurol Surg B Skull Base. 2023; 84(3): 225–31.
10. Song Z, Xu Y, Zhang X, You J, Wang H, Zheng R, et al. Application of a modified Costal cartilaginous framework in correction of severe saddle nose deformity. Aesthet Surg J. 2023; 43(8): 830–9.
11. Kuo P-H, Chang F-P, Chen C-H, Liao H-T. Saddle nose deformity in eosinophilic granulomatosis with polyangiitis. Joint Bone Spine. 2024; 91(6): 105765.
12. Harutyunyan A, Hakobyan G. Saddle nose deformity reconstruction with an allograft bone. Aesthetic Plast Surg. 2024; 48(23): 4839–47.
13. Rotenberg BW, Shapiro J, Zgardau A, Pourmomen B. How I do it: The role of nasal filler in managing cocaine-induced saddle nose deformity. Am J Cosmet Surg. 2025; (07488068251397587).
14. Pokala U, Poondru AR, Laxmi Santhi Swetha M S, Kavya V, Chukkapally S, Pokala N. A case of saddle nose deformity secondary to Lepromatous Leprosy. Indian J Otolaryngol Head Neck Surg. 2025; 77(2): 1014–8.
15. Alsiaghi YA, Al-Shoaibi MH, Al-Ajaly MY, Ghanem AM, Jowah HM. Saddle nose deformity reconstruction in Yemen: a prospective study of the diced cartilage fascia technique. Cureus. 2025; 17(2): e79319.
16. Alla I, Lorusso F, Gehrke SA, Tari SR, Scarano A. Absorbable dermal filler for saddle nose deformity associated with Wegener’s granulomatosis. J Cosmet Dermatol. 2025; 24(2): e70014.
17. Pham TT, Winkler AA, Gadkaree SK. Functional and cosmetic considerations in saddle nose deformity repair. Otolaryngol Clin North Am. 2025; 58(2): 325–41.
18. Kumar N, Jategaonkar G, Bansberg SF, Marino MJ, Lal D, Miglani A. Saddle nose deformity in granulomatosis with polyangiitis: Clinical and radiologic predictors from a multicenter cohort. Int Forum Allergy Rhinol. 2026; 16(1): 96–8.

19. Rabie AN, El Samny TA, Askoura AM, Desouky MS, Aty AMKA. The functional and aesthetic results of fibrin glue, platelet-rich plasma (PRP), and warm blood as a scaffold for diced cartilage in saddle nose deformity: a descriptive study. Facial Plast Surg. 2026; 42(1): 113–25.
20. Kumar N, Pace T, Gomes PL, Bansberg SF, Marino MJ, Lal D, et al. Quantitative analysis of nasal septal perforations associated with saddle nose deformity. Facial Plast Surg Aesthet Med. 2026; (26893614251408035): 26893614251408035.